The effect of process control agents and milling atmosphere on the structural changes of $Ti_{50}Cu_{27,5}Ni_{10}Zr_{10}Co_{2,5}$ master alloy during short time milling

IOP Conf. Series: Materials Science and Engineering **426** (2018) 012035 doi:10.1088/1757-899X/426/1/012035

The effect of process control agents and milling atmosphere on the structural changes of $Ti_{50}Cu_{27,5}Ni_{10}Zr_{10}Co_{2,5}$ master alloy during short time milling

T Miko[1], F Kristaly[2], K Bohacs[c], M Sveda[3], A Sycheva[4] and D Janovszky[5]

[1] University of Miskolc, Institute of Physical Metallurgy, Metalforming and Nanotechnology, Miskolc-Egyetemváros, Hungary
[2] University of Miskolc, Institute of Mineralogy and Geology, Miskolc-Egyetemváros, Hungary
[3] University of Miskolc, Institute of Raw Material Preparation and Environmental Processing, Miskolc-Egyetemváros, Hungary
[4] MTA-ME Materials Science Research Group, Miskolc-Egyetemváros, Hungary

E-mail: femmiko@uni-miskolc.hu

Abstract. Properties of powders made from $Ti_{50}Cu_{27,5}Ni_{10}Zr_{10}Co_{2,5}$ alloy, milled under different conditions for only 3600 s in total were investigated. For this purpose two different milling atmospheres and two different Process Control Agents (PCA) were tested: argon without PCA, air without PCA, argon combined with stearic acid, argon combined with petroleum spirit. Results showed that the size and shape of particles, and the microstrucutre and hardness of partcicles were highly depended on the milling conditions. According to XRD analysis, the maximal amorphous fraction has been achieved in the air atmosphere withouth PCA milled sample (57 wt. %) powder. However the extent of Fe contamination and weight loss during milling powder resulted bigger values. As a result, the optimal combination of morphology, contamination amount and weight lost level has been observed in the case of powder milled in argon atmosphere using stearic acid.

1. Introduction

Recently, the research of Ti-Cu-Ni based alloys has attracted much attention due to its high glass forming ability [1–3]. Compared with the crystalline alloys, the amorphous or nanocrystalline bulk alloy has excellent mechanical properties, due to the special mechanism of deformation and fracture arising from its structure [4, 5]. The high energy ball milling is an often used method to change the crystalline structure of metallic powder to amorphous/nanocrystalline microstructure. The two most important mechanisms during this process are the cold welding (particle adhesion and sticking) and the fracturing of the powder particles. The quality, the purity and the yield of milled powder strongly depends on the dominancy of either cold welding or fracturing. Bay [6] investigated the cold-welding mechanism, and concluded that for cold welded bonding to occur, plastic deformation of the powder particles is necessary, but shear welding also occurs with just local micro plastic deformation. The extent of cold welding is influenced by the milled powder properties (ductile or brittle) as well as the milling conditions (atmosphere, presence of liquids or lubricants). The ductile particles tend to be cold welded, but in case of the brittle phases, notable cold welding cannot occur. Changing the milling atmosphere or adding Process Control Agent (PCA, also referred to as lubricant or surfactant) to the mixture can also reduce

the effect of cold welding [7]. The PCA is adsorbed on the surface of the powder particles and minimizes cold welding [8]. One type of most commonly used PCA-s is solid (e.g. stearic acid), while others are liquid (e.g. hexane, methanol, or ethanol) [8]. Petroleum spirit however is not applied as PCA, one of the reasons to test its applicability, since it's easy to remove from the milled product and produces no contamination.

The atmosphere in which the milling process occurs is another important factor. Mechanical milling process is normally conducted under vacuum or in an inert atmosphere to prevent/minimize oxidation of the milled powder. The absence of oxide layer on the surface of broken particles causes that they can easily adhere to each other.

During ball milling, contamination is an additional process which is not easily prevented. In most cases, the aim is to decrease the extent of contamination also by using PCA-s. Contaminants will be nanoparticles of the milling equipment [8], which might be important regarding cold welding. Since ceramic particles will not be implied in mechanochemical reactions, metal contaminants (Fe, Cr or Mn) will tend to react with the milled alloys.

A reliable measure of cold welding activity is the powder yield [9] of milling, since the amount of unrecovered material has been adhered to the milling equipment. In the case of cold welding dominated milling, the powder yield is low, because big part of the powder attains to the balls and vial. If the powder yield is not high enough, then any PCA can be used to improve milling. It has been reported that after milling for 15h, only 50% of the powder was recovered if 2 wt% of polyethylene glycol was used, while almost 100% of the powder was recovered if stearic acid was used [9].

Four different milling conditions have been studied to highlight the high influence of ball milling parameters on the final products. The aim of this work is to compare the different milling atmospheres and some PCAs in terms of the particle size distribution, phase composition and microstructure.

2. Experimental conditions

Master alloy ingot with the compositions $Ti_{50}Cu_{27,5}Ni_{10}Zr_{10}Co_{2,5}$ (at. %) was prepared by vacuum induction melting of pure metal mixtures (min. 99.9 wt%). The ingot was grinded and fractioned to particle size below 320 μm for ball-milling. High energy ball milling was used with a Pulverisette 5 high-energy planetary ball-mill using a 250 ml hardened steel vial (63 HRC) and hardened steel balls (64 HRC) with a combination of Ø20 mm, Ø15 mm, Ø10 mm, Ø5 mm, and Ø2,5 mm, 10 pieces each. Ball to powder weight ratio and rotational speed were adjusted to 80:1 and 200 rpm, respectively. The angular velocity of the bowl and the supporting disc were calculated to be 231 and 200 rpm respectively. The initial weight of the powder was 6.4 g for each batch.

The micrographs of the powders were acquired with a Hitachi S-4800 scanning electron microscope (SEM) equipped with BRUKER AXS type energy-dispersive X-ray spectrometer (EDS) for elemental analysis. The particle size distribution of the ground material was determined by a Horiba LA-950 V2 type laser diffraction particle size analyser (LPSA) in distilled water (1 minute ultrasonic shaking, 1 ml of 50 g/l Na-pyrophosphate applied for dispersion). The as received and milled samples were examined by Bruker D8 Advance diffractometer (XRD) using Cu K□ radiation (40 kV, 40 mA), in parallel beam geometry obtained with Göbel mirror, equipped with Vantec-1 position sensitive detector (1° window opening), measured in the 2-100° (2θ) angular range, with 0.007° (2θ)/29 s speed. The specimen is rotated in sample plane during the measurement, to obtain data from the whole surface and to reduce in-plane preferred orientation effects. Quantitative results were obtained by combined use of Rietveld refinement and peak area calculation in TOPAS4, amorphous fraction was determined by fitting a broad peak (amorphous hump method). Microhardness measurements were performed by Instron Tukon 2100B equipment, applying a load of 10 g for 15 s for as milled powders.

3. Experimental results and discussion

3.1 Shape and size of the particles

SEM was used to visually follow the changes by milling. Coarse elongated-angular particles characterize the as received powder (Fig 1.a), with very different evolution depending on milling conditions (Fig 1.b,c,d,e). The volume distribution by LPSA of the as received powders particle shows that there are two modes x_{m1}= (72 μm), x_{m2}= (245 μm) (Fig.2), where the mode represents the most common particle size in a range. This bimodal character disappeared during milling except when using stearic acid PCA (Fig 1.c). In this case the higher mode decreased to x_{m2}= 78 μm, and the smaller mode decreased to x_{m1}= 15μm. The strangest behaviour was observed for Ar milled sample, resulting in large clustering (Fig 1.b) and strong adherence (Fig 2.) of fine particles.

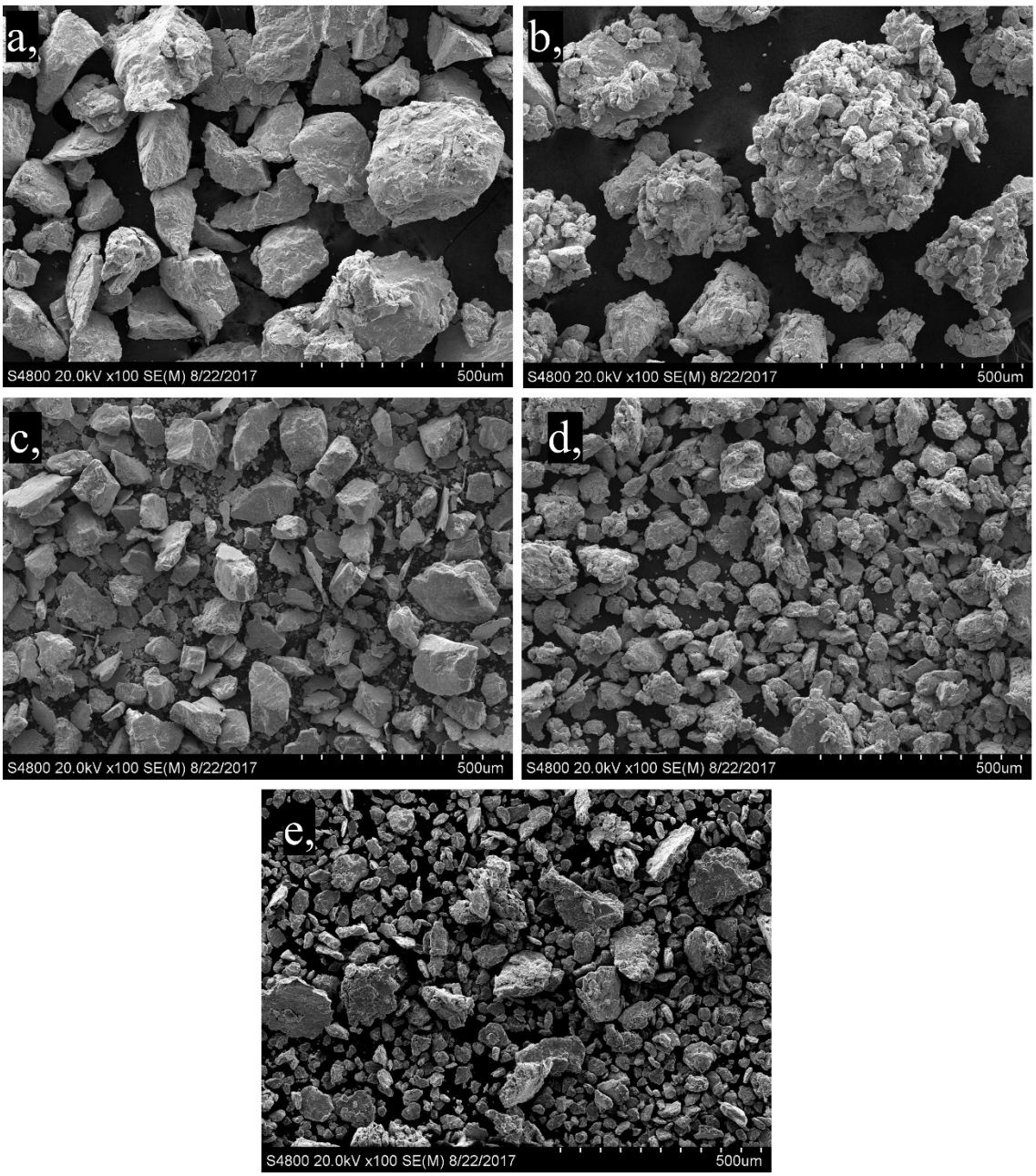

Figure 1. SEM images of as-received particles (a), and powders at 3600 s milling time: (b) argon (c) argon+ stearic acid, (d) petroleum spirit, (e) air.

Milling efficiency is reflected by LPSA values of D10, D50 and D90 (Fig 3.). The D50 value of Ar milled sample is practically the same as the stearic acid samples x_{m2}. However, in the argon milled

sample the smaller particle fraction does not appear separately, due to clustering and surface adherence. Using stearate acid, small particles generated by milling are maintained as individual. As shown by D_{50}=80 μm of Ar milling, this batch produced the smallest particle size decrease.

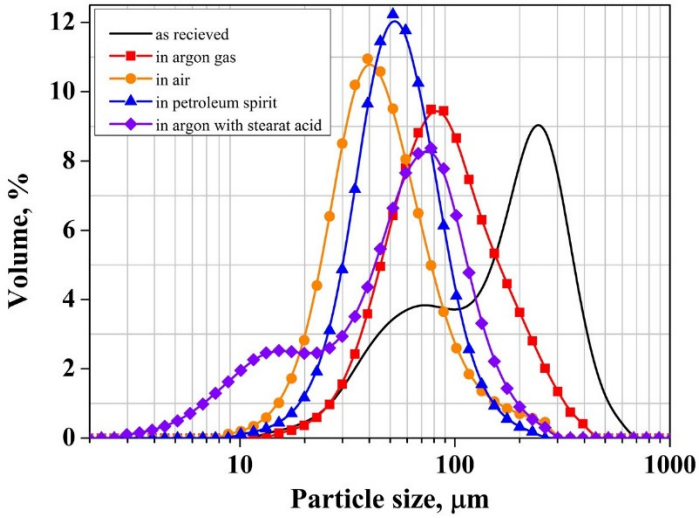

Figure 2. Volume distribution of as received and milled powders.

The smallest D_{50} value was measured in the air atmosphere milled sample (41 μm). This is because in absence of inert gas on the milling jar the cold welding was less significant. According to volume distribution of the air atmosphere and petroleum spirit milled sample, differences are minimal. However, based on SEM images, the shape and morphology is significantly different more platy and angular in air atmosphere milled, while more rounded and uniform in petroleum spirit milled sample (Fig 1 d, e).

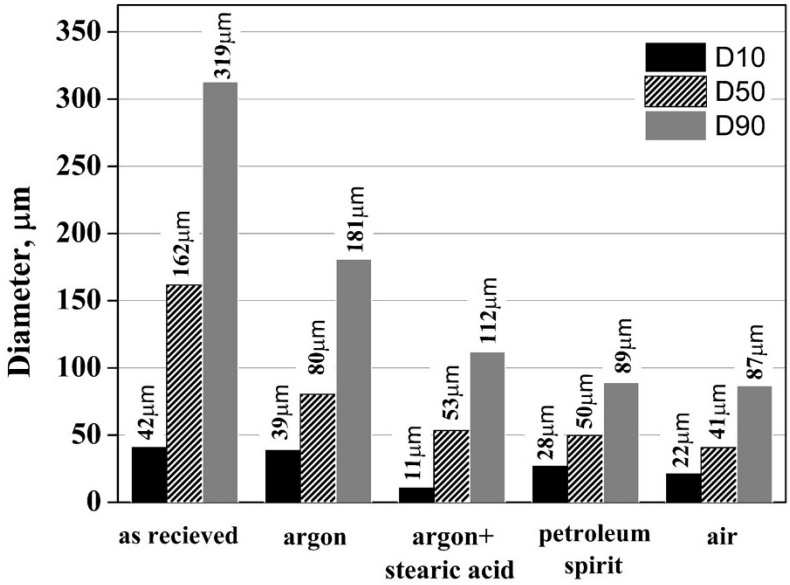

Figure 3. Effect of milling conditions on the average size of the particles

3.2. Contamination and yield properties

Fig. 4a shows the amount of powder before and after the milling processes, displaying also weight losses (wt %). The biggest difference between the weight of loaded and extracted mass is the case of dry milling with Ar atmosphere (-36 wt%). The reason for this is the significant degree of cold welding associated with adhering to the vial and ball surfaces. With a short (180 s) petroleum spirit milling step used after the 3600s milling time, significant quantity of milled powder was possible to recover from

the surface of balls and vial (Fig 4a). Therefore, the total weight loss just (-9 wt%) Significantly smaller losses occurred when we used stearic acid as a PCA in argon atmosphere (-4 and -0.3 wt%) respectively. The PCA blocked the adherence mechanism, and as can see in Fig 5.b, the surface of vial and balls remained clean even after the milling, against the case of argon (Fig 5.a,). The two other investigated cases resulted in very similar end, with ca. -3.5 wt% losses.

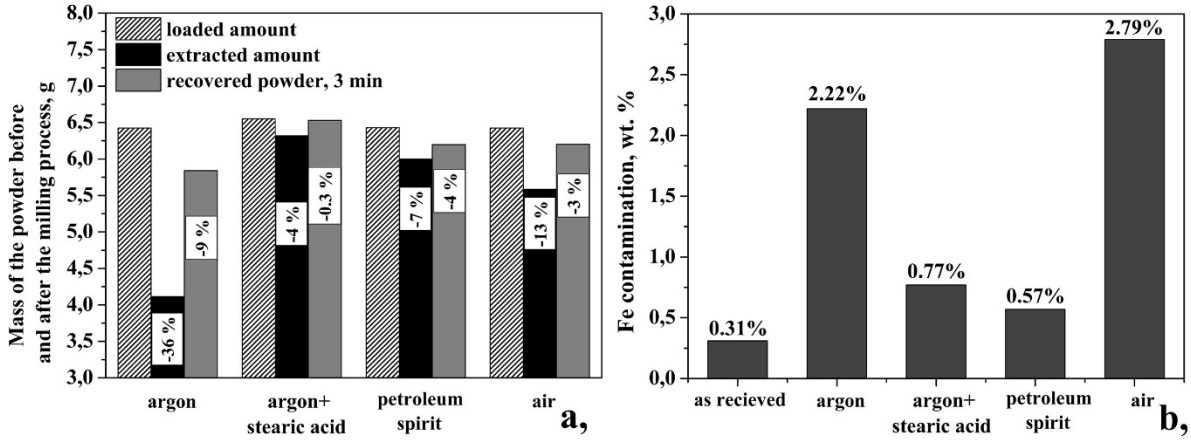

Figure 4. a, Weight loss during different milling conditions
b, Fe contamination in the case of different milling conditions (EDS)

Because we used steel vial and balls, the milled powder was contaminated with Fe during milling (Fig 4.b), highest value observed in air atmosphere without PCA (2.8 wt%), also significant in argon milled powder (2.2 wt%). The reason for this large quantity of Fe is the repeated cold welding and fracturing mechanism. The particles adhered to the balls and vial surface and then fractured from there by direct collision and relative friction, leading to transfer of atoms from the milling tool to the powder particles [7]. In the case of milling with stearic acid and petroleum spirit, the value of Fe contamination is much smaller, 0.8 wt% and 0.6wt% respectively. In these cases, the PCA-s act as lubricants between steel parts and alloy particles, preventing cold welding.

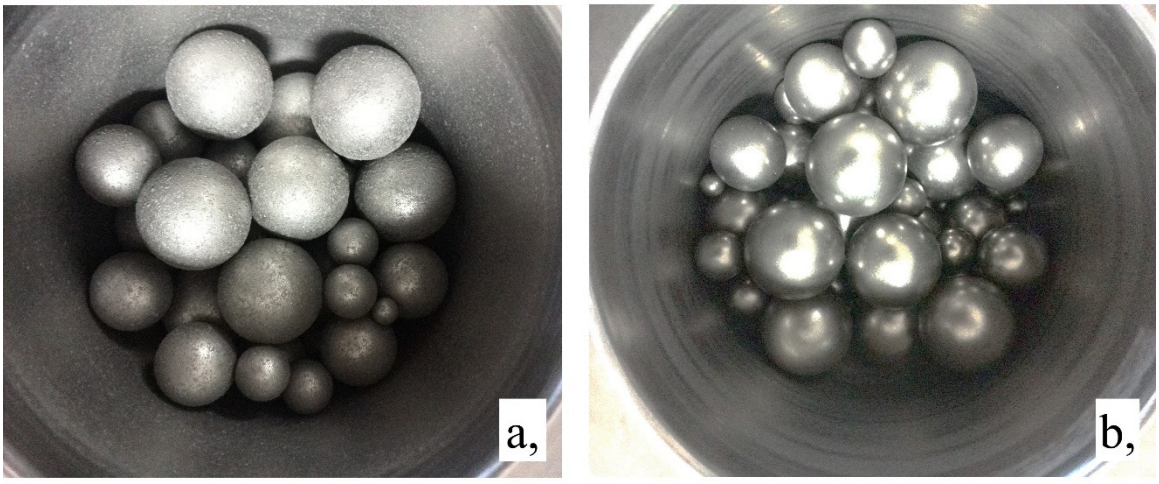

Figure 5. The surface of vial and balls after 3600 s milling a, in argon atmosphere without PCA b, argon atmosphere with 2 wt% stearate acid (PCA)

3.3 Microstructure and composition changes

Based on the XRD patterns eight different phases were identified in the as received $Ti_{50}Cu_{27,5}Ni_{10}Zr_{10}Co_{2,5}$ sample. In Fig 6.a, we have marked the main peaks of the major phases identified by Search/Match algorithm and Rietveld refinement. Transformations during milling can be followed

based on the changes of these peaks (Fig.6.b). Milling in air produced similar peak broadening to milling in argon and petroleum spirit, but Ti peaks remain more visible. The cubic Ti has been destroyed by milling.

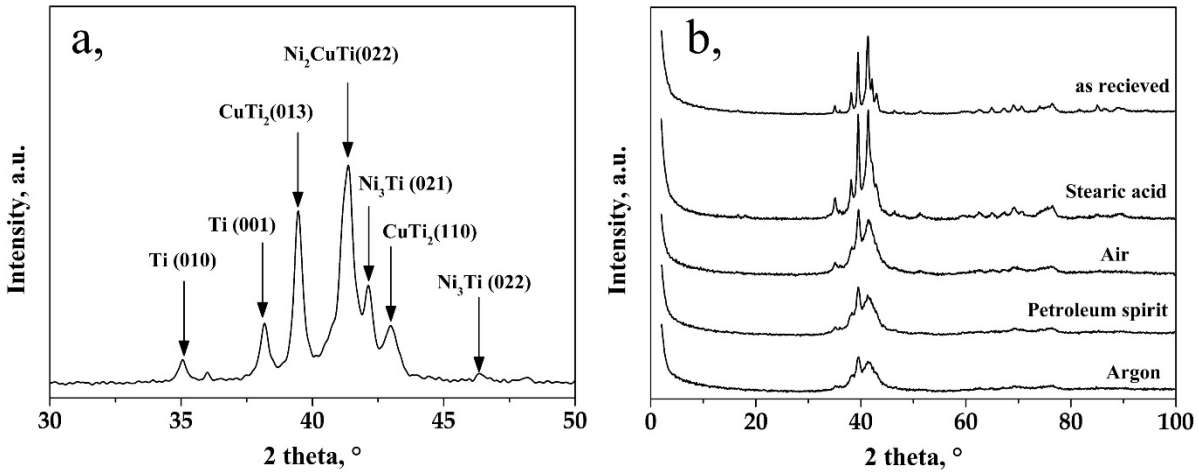

Figure 6. a, XRD pattern of $Ti_{50}Cu_{27,5}Ni_{10}Zr_{10}Co_{2,5}$ master alloy,
b, XRD patterns of powders with different milling agent

The change in the fraction of phases shows a very interesting trend as a function of the milling condition. The weight fractions of the different phases are summarized in Table 1. From the eight initial phases amount of five decreases or they disappear (Ti, $CuTi_2$, Ni_3Ti_3, Ni_2CuTi, Ti(Fm-3m)), while amount of three increases ($CuTi_3$, $Cu(Ni_{0.7}Cu_{0.3})Ti_2$, $Cu_{0.5}Ni_{0.5}Ti$). Amorphous phases arise in all samples, regardless the milling conditions, but their amount varies according to atmospshere and PCA-s.

Table 1. Fraction of crystalline and amorphous phase of the as received and milled powder

Phase name	space group	Crystalline size, nm				
		as recieved	Milling atmosphere/PCA			
			Air	Argon	Argon+stearic acid	Petroleum spirit
Ti	P63/mmc	11.5	3.7	4.3	6.4	8.4
$CuTi_3$	P4/mmm	2.8	16.7	13	19.4	10.7
$Cu(Ni_{0.7}Cu_{0.3})Ti_2$	Pmmb	1.2	2	1.2	5	2.1
$CuTi_2$	I4/mmm	35.3	5.5	6.9	3	7.5
Ti (Fm-3m)	Fm-3m	5.1	-	-	-	-
Ni_3Ti_3	P63/mmc	10	0.7	0.6	0.8	1.3
$Cu_{0.5}Ni_{0.5}Ti$	Pmmb	4.1	9.8	12.9	25.3	11.8
Ni_2CuTi	Fm-3m	30	4.6	6.3	2.1	6.2
amorphous	-	0	57	55	38	52

The phase evolution of powder caused by high energy ball-milling was plotted as function of different milling condition, which can be seen in Fig. 7. Compared to the four difference milled powders, the quantity of phases in argon+stearic acid sample significantly differs from the others. Using this milling condition the value of amorphous phase is the smallest (38 wt%), but the amount of $CuTi_3$ (19.4 wt%) and $Cu_{0.5}Ni_{0.5}Ti$ (25.3 wt%) are the biggest, compared with the other samples.

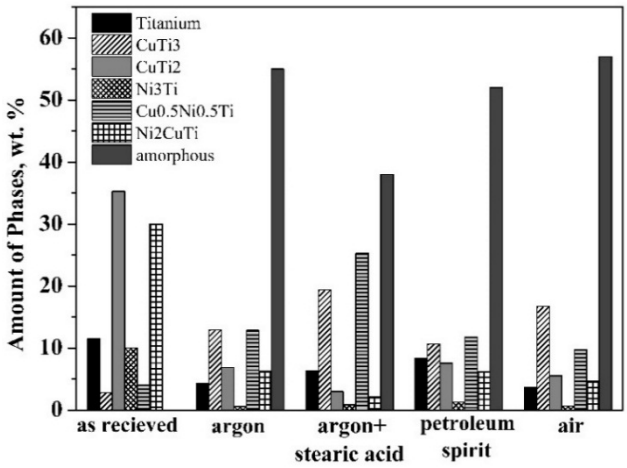

Figure 7. Fraction of crystalline and amorphous phases of the as received and milled powders

Measurement of the crystallite size in the powders is also very important since the phase constitution and transformation characteristics appear to be critically dependent on the crystallite size. The crystallite size decreases significantly due to the milling processes (Fig. 8.). The smallest amount of decreasing is in the case of stearic acid. This is because the low friction, the milling balls and the powder particles are mainly just rolling on the inner wall of the bowl. The plastic deformation of powder particles is low, so the surface of the flake shaped particles becomes very smooth (Fig. 1. c) compared to all other investigated cases.

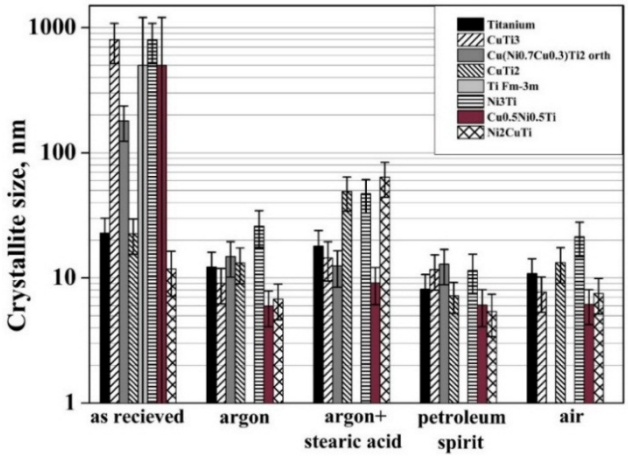

Figure 8. Crystallite size of as received and milled powders.

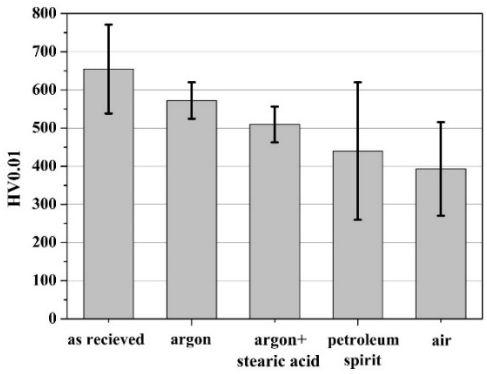

Figure 9. Hardness of the different condition milled powder particles

The measured hardness values of the different powder particles are shown in Fig. 9. The as received

sample has the biggest mean hardness (655 $HV_{0.01}$) compared to the hardness of milled powders. However, the standard deviation is significant, because it contains many different phases besides the brittle intermetallic phases, contains also ductile parts, like Ti structures. The particle size of powder is large compared to the all other milled powder. Hardness of each milled powder samples are below to the as received sample. The tendency of hardness lowering is equal to the decreasing of mean particle size (Fig. 3.). The smallest hardness decrease was measured in the Ar milled sample (572 $HV_{0.01}$), while the biggest decrease is measured in the air atmosphere milled sample (393 $HV_{0.01}$).

4. Conclusion

In this study the effect of different milling atmosphere and PCA was studied on $Ti_{50}Cu_{27,5}Ni_{10}Zr_{10}Co_{2,5}$ alloy. During only 3600 s milling time, the particles size as well as the crystallite size and amorphous content went through a big change.

Use of petroleum spirit and stearic acid considerably reduces the Fe contamination compared to the case of milling without any PCA. The best yielding properties of the milled powder were measured using stearic acid (96%). The worst yielding properties of the milled powder measured milling in argon atmosphere without any PCA (64 wt %). Using a short (3 min) wet milling with petroleum spirit, this value increases to 91 wt%. The content of Fe and Cr impurities in the milled powder increased when the cold-welding process is dominant, Ar and air without PCA.

Milling with petroleum spirit and stearic acid the Fe contamination and the weight loss was much smaller than in the cases without any surfactant. The biggest amorphous content obtained milling without any PCA and inert atmosphere. Using stearic acid obtained the smallest amorphous content. The amorphization process of structure is not as rapid with use of stearic acid as PCA, then in the other investigated cases.

Acknowledgements

"The described article/presentation/study was carried out as part of the GINOP-2.3.2-15-2016-00027 "Sustainable operation of the workshop of excellence for the research and development of crystalline and amorphous nanostructured materials" project implemented in the framework of the Szechenyi 2020 program. The realization of this project is supported by the European Union."

References

[1] Pan Gong, Lei Deng, Junsong Jin, Sibo Wang, Xinyun Wang, Kefu Yao 2016 Review on the Research and Development of Ti-Based Bulk Metallic Glasses *Metals*; 264

[2] Tao Chang, Akihisa Inoue 1998 Thermal and Mechanical Properties of Ti-Ni-Cu-Sn Amorphous Alloys with a Wide Supercooled Liquid Region before Crystallization, *Materials Transaction*, 1001 to 1006.

[3] Jianli Wang, Baozhong Liu, Lidong Wang, Yaoming Wu, Limin Wang 2008 Glass formation ability and mechanical properties of Ti40Cu40Zr10Ni10 alloy, Journal of Non-Crystalline Solids *Journal of Non-Crystalline Solids* 3653–3658

[4] Christopher A. Schuh, Todd C. Hufnagel, Upadrasta Ramamurty 2007 Mechanical behavior of amorphous alloys Review on the Research and Development of Ti-Based Bulk Metallic Glasses *Acta Materialia* 4067–4109

[5] Y.C. Kim, W.T. Kim, D.H. Kim 2004 A development of Ti-based bulk metallic glass *Materials Science and Engineering* 127–135

[6] N. Bay 1986 Cold welding. Part 1: Characteristics, Bonding Mechanism, Bond Strength, *Metal Construction*, 369-372

[7] G. Cipolloni, M. Pellizzari, A. Molinari, M. Hebda, M. Zadra 2015, Contamination during the high-energy milling of atomized copper powder and its effects on spark plasma sintering, *Powder Technology* 51–59

[8] C. Suryanarayana 2001 Mechanical alloying and milling, *Progress in Materials Science* 1-184.

[9] Lai MO, Lu L 1998 Mechanical alloying Boston, MA: Kluwer Academic Publishers